Extended Abstracts of the 2011 International Conference on Solid State Devices and Materials, Nagoya, 2011, pp1409-1410

Epitaxy of Spinel Zn_2TiO_4 (111) on GaN (001) for MOS Application

Sheng-Wen Fu, Jhih-Cheng Wu, Chu-Yun Hsiao, Kuang-Teng Hung, Shih-Hsiung Wu, Hui-Ju Chen, Hsuan-Ta Wu, and Chuan-Feng Shih*

Department of Electrical Engineering, National Cheng Kung University, 1 University Road, Tainan, 70101, Taiwan
Phone: +886-6-2757575 ext.62398 Fax:+886-6-2080687 E-mail: cfshih@mail.ncku.edu.tw

1. Introduction

The pursuit of high-permittivity gate oxides for use in GaN-based metal-semiconductor field-effect-transistors (MES-FETs), hetero-junction FETs (HFETs), and high-electron-mobility transistors (HEMTs) has attracted great attention in the past few years [1,2]. However, several factors have limited the progress. For example, a poor Schottky contact is formed when metal comes into direct contact with the semiconductor directly, generating a leakage current. Metal-oxide-semiconductor FETs (MOS-FETs) and MOS-HFETs have reportedly been formed by introducing a thin oxide or nitride layer, such as AlN, Ga_2O_3, SiO_2, Si_3N_4, Al_2O_3, HfO_2, MgO, or Ta_2O_5 to overcome the leakage problem [3-9]. However, most studies of high-k layers for GaN-based MOS have focused on the deposition of few metal oxides [1-10], ignoring the fact that many ceramic materials have such advantages as high dielectric constant, high thermal stability, and low dielectric loss. Spinel, which consists of face-centered cubic oxygen and cations that occupy octahedral or tetrahedral sites, can also grow epitaxially on GaN. The close-packed oxygen plane in spinel should have some epitaxial relationship with GaN (001).

Zn_2TiO_4 is an inverse spinel that has been utilized in various applications, including sensors, pigment, catalyst, and microwave dielectrics [11,12]. This work investigates the epitaxy of zinc titanate (Zn_2iO_4) and the use as a gate oxide of a GaN-based MOS capacitor. X-ray diffraction (XRD) and high-resolution transmission electron microscopy were used to determine the preferred orientation, crystallinity, and epitaxy relationship of the Zn_2TiO_4 films. Finally, the dielectric property of the Zn_2TiO_4/GaN-based capacitor was investigated.

2. Experimental details

Sputtering was conducted at an rf-power of 125 W and a working pressure of 2×10^{-3} torr following pre-sputtering for 15 min. Pure argon or mixed argon/oxygen (5 sccm/5 sccm) gases were separately introduced to the vacuum chamber for sputtering. The Zn_2TiO_4 thin film was ~30 nm-thick. The n-type GaN was grown on (0001) sapphire with a thickness of ~4 μm and a doping concentration of 1×10^{18} cm^{-3}. The films were post-annealed by rapid thermal annealing (RTA). The structure and the orientation of the Zn_2TiO_4 thin films were characterized by X-ray diffractometry (XRD) using θ-2θ, glazing angle (Siemens/D5000). An Al gate electrode was formed by thermal evaporation. HR-TEM (JEOL/JEM-2100) was used to obtain lattice image at the interface between GaN and Zn_2TiO_4. The electrical properties of the fabricated MOS capacitors were determined by measuring high-frequency capacitance-voltage (C-V) curves using an Agilent E4980A impedance analyzer.

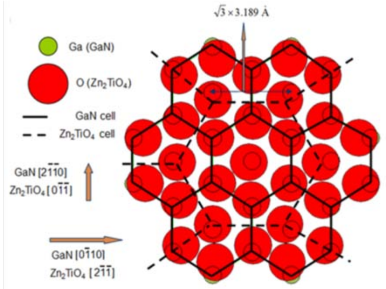

Figure 1 Epitaxial relationship in Zn_2TiO_4 (111)/GaN (001) interface.

3. Results and Discussion

Figure 1 plots the atomic stacking sequence and epitaxial relationship between Zn_2TiO_4 (111) and GaN (001). The plot is based on the fact that the oxygen in Zn_2TiO_4 (111) and Ga (or N) in GaN (001) have the same symmetry and similar lattice constants. Therefore, the lattice constant of Zn_2TiO_4 is estimated to be 6% smaller than that of GaN. Figure 2(a) displays XRD patterns of samples that were deposited by sputtering in an argon/oxygen mixture. This observation supports the assumed atomic stacking sequence that was displayed in Fig. 1. Glazing-angle XRD (GIXRD) patterns in Figs. 2(b) correspond to Figs. 2(a). Generally, GIXRD signals may be absent for one of the two possibilities: the film is amorphous or the film is highly-preferred. Comparing the θ-2θ XRD and GIXRD patterns in Figs. 2(a) and (b) reveals that the GIXRD signals of the RTA-treated samples were absent, but the θ-2θ signals of the (111) planes of those samples were strong, indicating that these films had a highly-preferred orientation. Both GIXRD and θ-2θ spectra of samples that were prepared in pure-argon included diffraction peaks, indicating that they are poly-crystalline.

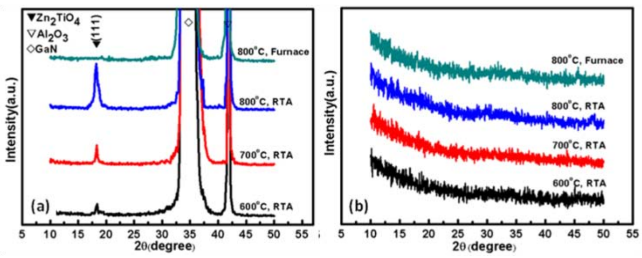

Figure 2 (a) XRD θ-2θ and (b) GIXRD profiles of Zn_2TiO_4 with different annealing temperatures. Zn_2TiO_4 prepared in argon/oxygen. Holding time and ramping rate for RTA are 3 min and 10 ^{o}C/s.

Figures 3(a) and (d) display the selected-area diffraction (SAD) patterns and the high-resolution TEM images at the Zn_2TiO_4/GaN interface. The zone axes of the GaN and Zn_2TiO_4 layers were $[100]$ and $[1\bar{2}1]$, respectively.

Figures 3(a) and (b) show the SAD and HR-TEM images of Sample A. The GaN (001) and Zn_2TiO_4 (111) were coherent and parallel. Therefore, the TEM investigation suggested that RTA and the use of oxygen in sputtering were associated with the enhancement of the Zn_2TiO_4 (111) preferring-orientation. The epitaxial relationship was determined from both the XRD and TEM observations to be Zn_2TiO_4 (111)|| GaN (001), Zn_2TiO_4 $(20\bar{2})$|| GaN (110), and Zn_2TiO_4 $[2\bar{1}\bar{1}]$|| GaN $[0\bar{1}\bar{1}0]$.

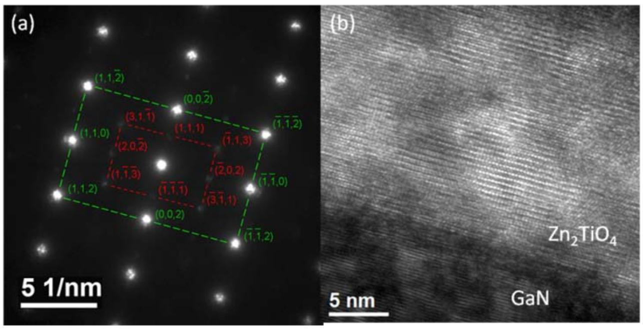

Figure 3 TEM SAD patterns and lattice images. (a) and (b) are are for Zn_2TiO_4 prepared in pure argon and RTA at 800 °C for 3 min.

Figure 4 plots the C-V curve of the (111)-preferring Zn_2TiO_4/n-GaN-based MOS diode at 2MHz. The relative dielectric constant (ε_{ox}=18.85) was calculated from the accumulation capacitance (~115 pF) using $C_{ox}= \varepsilon_{ox}\,\varepsilon_0 A / t_{ox}$, where ε_0 is the permittivity of vacuum; t_{ox} denotes the thickness of the oxide, and A = 9.75x10^{-2} mm^2 is the area of the capacitors. Notably, the measured dielectric constant of the Zn_2TiO_4 thin film is the highest ever reported in literature. Moreover, the epitaxy of the Zn_2TiO_4 effectively modified the interface properties and improved the dielectric properties of the ceramic oxide. The amorphous and polycrystallinc Zn_2TiO_4 films had lower permittivity and larger leakage current than the epitaxial Zn_2TiO_4 film. Relative to the simulated (ideal) C-V curve, which assumes zero interface traps, the experimental C-V curve was somewhat stretched-out because of the interfacial traps. The interfacial trap density (8.5×10^{11} cm^{-2}/eV) was

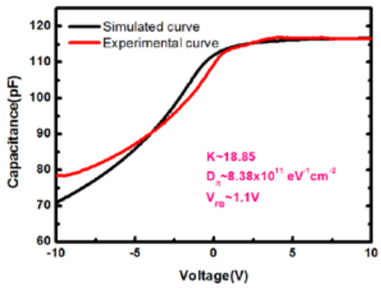

Figure 4 Measured and simulated C-V curve for (111)-preferring Zn_2TiO_4/GaN MOS capacitor.

calculated from the simulated (ideal) and experimental C-V curves using the Terman method [13,14]. A small flat-band voltage shift ~1.1 V was observed. The relative dielectric constant was smaller than that of the bulk material (~22), because the annealing temperature was intentionally kept below 800 °C to prevent coarsening or damaging of the GaN.

4. Conclusion

Spinel Zn_2TiO_4 thin films were epitaxially grown on GaN by rf-sputtering. The oxygen during sputtering and RTA enhanced the epitaxy of Zn_2TiO_4(111) on GaN (001). The epitaxial relationship was determined by the XRD and transmission electron microscopy: Zn_2TiO_4 (111)|| GaN (001), Zn_2TiO_4 $(20\bar{2})$|| GaN (110), and Zn_2TiO_4 $[2\bar{1}\bar{1}]$|| GaN $[0\bar{1}\bar{1}0]$. The epitaxial Zn_2TiO_4 effectively modifies the interface properties and improves the dielectric properties of the ceramic oxide. Finally, the relative permittivity, interfacial trap density and the flat-band voltage of the Zn_2TiO_4/GaN-based MOS capacitor was found to ~ 18.9, 8.38×10^{11} eV^{-1}cm^{-2}, and 1.1 V, respectively.

Acknowledgements

This work was supported by the National Science Council under contract No. NSC 99-2622-E-006-019-CC3 and the Center for Micro/Nano Science and Technology.

References

[1] C. Q. Chen, J. P. Zhang, V. Adivarahan, A. Koudymov, J. Fatima, G. Simin, J. Yang, and M. A. Khan, *Appl. Phys. Lett.*, **82** [25], 4593-5 (2003).

[2] Y. Irokawa, B. Luo, F. Ren, C. C. Pan, G. T. Chen, J. I. Chyi, S. S. Park, Y. J. Park, and S. J. Pearton, *Electronchem.Solid-State Lett.*, **7** [1], G8-10 (2004).

[3] C. T. Lee, H. W. Chen, and H. Y. Lee, *Appl. Phys. Lett.*, **82** [24], 4304-6 (2003).

[4] K. Matocha, R. J. Gitmann, and T. Paul Chow, *IEEE Trans. Electron Device*, **50** [5], 1200-4 (2003).

[5] S. Arulkumaran, T. Egawa, H. Ishikawa, T. Jimbo, and M. Umeno, *Appl. Phys. Lett.*, **73** [6], 809-11 (1998).

[6] Y. C. Chang, H. C. Chiu, Y. J. Lee, M. L. Huang, K. Y. Lee, M. Hong, Y. N. Chiu, J. Kwo, Y. H. Wang, *Appl. Phys. Lett.*, **90** [23], 232904-1-3 (2007).

[7] H. Cho, K. P. Lee, B. P. Gila, C. R. Abernathy, S. J. Pearton, and F. Ren, *Solid-State Electron.*, **47** [9], 1597-600, (2003).

[8] T. Adan, J. Kolodzey, C. P. Swann, N. W. Tsao, and J. F. Rabolt, *Appl. Sur. Sci.*, **175-6**, 428-35, (2001).

[9] L. W. Tu, W. C. Kuo, K. H. Lee, P. H. Tsao, C. M. Lai, A. K. Chu, and J. K. Sheu, *Appl. Phys. Lett.*, **77** [23], 3788-90 (2000).

[10] R. Kim, Y. Kim, and J. W. Park, *J. Mater. Sci.*, **36**, 1469-73 (2001).

[11] C. F. Shih, W. M. Li, M. M. Lin, K. T. Hong, C. Y. Hsiao, and C. L. Lee, *Electrochem. Solid-State Lett.*, **11** [12] K105-K108 (2008).

[12] C. F. Shih, W. M. Li, M. M. Lin, and K. T. Hung, *J. Electrochem. Soc.*, **156** [1] E13-E17 (2009).

[13] L. M. Terman, *Solid-State Electron*, **5**, 285-99 (1962).

[14] E. H. Nicollian and J. R. Brews, *MOS Physics and Technology*, 1st Edition, Wiley, pp.328 (1982).